Published OnlineFirst November 5, 2020; DOI: 10.1158/0008-5472.CAN-20-1480

PWD/Ph-Encoded Genetic Variants Modulate the Cellular Wnt/β-Catenin Response to Suppress *Apc*^{Min}-Triggered Intestinal Tumor Formation

Alexandra L. Farrall[1,2], Matthias Lienhard[1], Christina Grimm[1,3], Heiner Kuhl[1,4], Susanna H.M. Sluka[1], Marta Caparros[1], Jiri Forejt[5], Bernd Timmermann[1], Ralf Herwig[1], Bernhard G. Herrmann[1,6], and Markus Morkel[7]

ABSTRACT

Genetic predisposition affects the penetrance of tumor-initiating mutations, such as APC mutations that stabilize β-catenin and cause intestinal tumors in mice and humans. However, the mechanisms involved in genetically predisposed penetrance are not well understood. Here, we analyzed tumor multiplicity and gene expression in tumor-prone *Apc*$^{Min/+}$ mice on highly variant C57BL/6J (B6) and PWD/Ph (PWD) genetic backgrounds. (B6 × PWD) F1 *APC*^{Min} offspring mice were largely free of intestinal adenoma, and several chromosome substitution (consomic) strains carrying single PWD chromosomes on the B6 genetic background displayed reduced adenoma numbers. Multiple dosage-dependent modifier loci on PWD chromosome 5 each contributed to tumor suppression. Activation of β-catenin–driven and stem cell–specific gene expression in the presence of *Apc*^{Min} or following APC loss remained moderate in intestines carrying PWD chromosome 5, suggesting that PWD variants restrict adenoma initiation by controlling stem cell homeostasis. Gene expression of modifier candidates and DNA methylation on chromosome 5 were predominantly *cis* controlled and largely reflected parental patterns, providing a genetic basis for inheritance of tumor susceptibility. Human SNP variants of several modifier candidates were depleted in colorectal cancer genomes, suggesting that similar mechanisms may also affect the penetrance of cancer driver mutations in humans. Overall, our analysis highlights the strong impact that multiple genetic variants acting in networks can exert on tumor development.

Significance: These findings in mice show that, in addition to accidental mutations, cancer risk is determined by networks of individual gene variants.

Introduction

Cancers are driven by genetic mutations and epigenetic alterations arising in individual somatic cells, primarily adult stem cells. Loss of the tumor suppressor APC is the most frequent initiating mutation in human colon and mouse intestinal cancer (1), preventing the destruction of nuclear β-catenin, thereby stabilizing stem cell fate (2).

The sequential acquisition of multiple mutations in oncogenes or tumor suppressors during a lifetime that eventually leads to cancer has been considered as a matter of "bad luck" (3). In this model, cancer occurs via DNA replication errors generating cancer driver mutations, which is a random process related to the number of stem cell divisions in the tissue. In familial cancer, high-penetrance susceptibility mutations provide a cancer driver allele already in the germline, thereby strongly increasing cancer risk. In colon cancer, inherited heterozygous mutations in the *APC* tumor suppressor gene cause familial adenomatous polyposis (4–6).

Adding complexity to this simple stochastic model, studies in human individuals, twins, and populations have demonstrated that the incidence of sporadic (nonfamilial) cancers also has a genetic component (7, 8). For instance, monozygotic twins were found to have a higher than random chance of developing cancer of the same organ, including the colorectum (9). Chances of developing sporadic cancer may thus partly depend on largely undefined sets of low-penetrance alleles of multiple genes, each making some contribution to the individual lifetime risk of developing cancer.

The assessment of cancer incidence in mice with inbred genetic backgrounds provides an opportunity to determine genetic factors and mechanisms modifying cancer susceptibility (10–13). Commonly, these modifier genes are identified by comparing defined, but different, inbred genomes in cancer models carrying a high-penetrance allele, resulting in high tumor multiplicity per animal. The most common mouse model for colon cancer is the *Apc*^{Min} mouse carrying a heterozygous germline mutation in *Apc* (14, 15). On a C57BL/6 inbred genetic background, *Apc*$^{Min/+}$ mice can develop more than a 100 intestinal adenomas by the age of 3 months. Environmental factors,

[1]Max Planck Institute for Molecular Genetics, Berlin, Germany. [2]College of Medicine and Public Health, Flinders University, Adelaide, South Australia, Australia. [3]Department of Translational Epigenetics and Tumor Genetics, University Hospital Cologne, Cologne, Germany. [4]Leibniz-Institute of Freshwater Ecology and Inland Fisheries, Department of Ecophysiology and Aquaculture, Berlin, Germany. [5]Institute of Molecular Genetics, Academy of Sciences of the Czech Republic, Vestec, Prague, Czech Republic. [6]Charité – Universitätsmedizin Berlin, corporate member of Freie Universität Berlin, Humboldt-Universität zu Berlin, and Berlin Institute of Health, Institute for Medical Genetics, Berlin, Germany. [7]Charité – Universitätsmedizin Berlin, corporate member of Freie Universität Berlin, Humboldt-Universität zu Berlin, and Berlin Institute of Health, Institute of Pathology, Berlin, Germany.

Note: Supplementary data for this article are available at Cancer Research Online (http://cancerres.aacrjournals.org/).

A.L. Farrall and M. Lienhard contributed equally as co-first authors of this article.

B.G. Herrmann and M. Morkel contributed equally to this article.

Corresponding Authors: Markus Morkel, Charité Universitätsmedizin Berlin, Charitéplatz 1, Berlin 10117, Germany. Phone: 4930-450-536107; E-mail: Markus.Morkel@charite.de; and Bernhard G. Herrmann, Max Planck Institute for Molecular Genetics, Ihnestrasse 63, 14195 Berlin. Phone: 4930-8413-1409; E-mail: herrmann@molgen.mpg.de

Cancer Res 2021;81:38–49

doi: 10.1158/0008-5472.CAN-20-1480

Published OnlineFirst November 5, 2020; DOI: 10.1158/0008-5472.CAN-20-1480

such as the diet and the gut microbiome, also affect tumor multiplicity (16). Multiple loci have been identified that modify tumor incidence of *Apc*$^{Min/+}$ mice (17). However, how modifier candidates interact with the cell signaling network controlling intestinal homeostasis has not been investigated in detail.

Here, we employed C57BL/6J (B6) and PWD/Ph (PWD) chromosome substitution (consomic) mouse lines as a rich source of genetic variation (18). We found that PWD chromosomes encode multiple modifiers of Min with tumor-protective effects. We show that the expression of many PWD and B6 alleles, as well as patterns of DNA methylation, are *cis*-controlled and preserved in offspring F1 mice. We provide evidence that differences in intestinal tumor multiplicity between B6 and PWD mice correlate with the control of intestinal Wnt/β-catenin activity. Our study, therefore, provides genetic evidence for the inheritance of individual cancer risks via modifier gene variants controlling cell signaling networks.

Materials and Methods

Mice

C57BL/6J (B6, The Jackson Laboratory) mice were maintained by backcrossing to C57BL/6JOlaHsd (Harlan). PWD mice and consomic strains were obtained from the Academy of Sciences of the Czech Republic (Vestec, Czech Republic) and imported to the animal facility of the MPIMG by embryo transfer. Animals were housed at a 12-hour/12-hour light/dark cycle and fed *ad libitum*. Mice were genotyped for *Apc* wild-type and Min alleles from tail DNA. Genotyping for B6 and PWD sequences on chromosome 5 was done using a panel of 36 polymorphic SNP markers, as published previously (18).

Mice of both sexes were euthanized and dissected at the age of 15–19 weeks, and intestinal tumors were counted under a stereomicroscope. Tissues for IHC and sequencing were excised from the ileum. For sequencing experiments, *Apc*$^{+/+}$ and *Apc*$^{Min/+}$ intestinal samples and adenomatous tissues of male mice were sampled from B6, heterozygous B6/PWD chr5 consomic, and homozygous PWD chr5 consomic genetic backgrounds in triplicate. Mouse work was approved by the Berlin State Office for Health and Social Affairs (LAGeSo, Berlin, Germany) under permit ZH120.

Histology and sample preparation

For histology, tissues were fixed in 4% formaldehyde, dehydrated via a graded ethanol series, embedded in paraffin, and sectioned at 4 μm. RNA ISH was performed on rehydrated paraffin sections using 800 ng/mL digoxigenin-labeled *Olfm4* antisense probes. Signals were detected using anti-digoxigenin-Fab fragments coupled to alkaline phosphatase (Roche) and a nitro blue tetrazolium and 5-bromo-4-chloro-3′-indolyphosphate chromogenic reaction. Primer sequences flanking the *in situ* probe were 5′-GGA CCT GCC AGT GTT CTG TT-3′ and 5′-TAA TAC GAC TCA CTA TAG GGC CCC CAT TGT ACC AAT TCA C-3′. Lysozyme IHC was performed using anti-LYZ antibody (Abcam, ab108508; 1:500). For RNA/DNA extraction, mouse normal and adenoma tissue samples were processed in RLT/1 mmol/L DTT (Qiagen) using a Tissue Lyser (Qiagen) for 2 × 2 minutes; frequency, 20. DNA and RNA were isolated using the Allprep DNA/RNA Mini Kit (Qiagen). DNAse digest of the RNA was performed according to the manufacturer's instructions. Nucleic acid concentrations were measured with a NanoDrop Photometer (Implen) or Qubit Fluorometer (Invitrogen) and quality was assessed on an agarose gel (for DNA) or a 2100 Bioanalyzer (Agilent Technologies) for RNA.

Organoid culture

Intestinal organoids were cultured according to procedures published previously (19) in Matrigel (Corning). Normal intestinal organoid medium contained the growth factors, EGF, Noggin, and R-Spondin. Adenoma cultures were selected for spheroid formation by omission of R-Spondin.

Library preparations and methylated DNA immunoprecipitation

For RNA sequencing (RNA-seq), 4 μg total RNA was depleted for ribosomal RNA using RiboMinus Eukaryote Kit for RNA-seq (Invitrogen), and used for generation of single-end RNA-seq libraries, as described previously (20). cDNA libraries were size selected (150–200 bp) on a 2% agarose gel, and purified using the Qiaquick Gel Extraction Kit (Qiagen). DNA sequencing was performed on NextSeq 500 Sequencers (Illumina) with 2 × 150-bp read lengths, using 500 bp insert sizes and several mate-pair libraries without size selection with sizes ranging from 3 to 15 kb. Methyl-DNA immunoprecipitation and sequencing were performed as published previously (21), using a GAIIx Sequencer (Illumina) and Illumina 1.5 and 1.6 pipelines.

Assembly of the PWD genome

DNA reads were assembled in a hybrid approach, using IDBA-UD assembler (22), followed by NEWBLER v3 (Roche/454) and SSPACE2 scaffolding (23, 24), yielding a total contig length of 2.351 gigabases and N50 length of 10,731 bp. We used Platanus gap close (25) and SOAPdenovo's GapCloser (26) for an initial draft assembly spanning 2.535 gigabases, corresponding to 92.8% of the mouse genome size with an N50 scaffold length of 2.46 megabases. Comparing these scaffolds to mm10 reference identified 573 breaks of colinearity with an average 340-fold mate-pair physical coverage. A total of 242 breaks supported by less than 75-fold coverage were considered potential assembly errors, resulting in scaffold splits. Scaffolds were combined to superscaffolds using genome alignment to mm10 by LAST aligner (27) and Ragout (28). Ultimately, we assembled 2.57 gigabases of PWD genomic sequence, corresponding to 94% of mm10 mouse reference genome, including 97% of reference chromosome 5 by eight PWD scaffolds, ranging from 100 kilobases to 78.94 megabases (Supplementary Fig. S1A).

Quantitative trait loci analysis

Quantitative trait loci (QTL) analysis was performed using R/qtl (29) after converting polymorphic markers to genetic positions (30). We performed QTL analysis with tumor load phenotype and genotype data using the EM algorithm and permutation analysis ($n = 10.000$ permutations) to determine significance.

Mixed reference alignment strategy for B6 and PWD genomes

To enable direct comparison of chromosome 5 sequencing data from B6 and PWD genomes, mm10 reference sequence was fragmented to 250-base windows and aligned to chr5 PWD scaffolds with Last alignment tool, identifying corresponding PWD windows for 564,283 of 607,338 mm10 B6 windows (93%). A total of 543,242 windows (89%) were affected by sequence variants, with a median of nine variant bases. To avoid bias from unequal maturity of the B6/mm10 and PWD assemblies when aligning RNA or MeDIP sequence reads, we considered only reads that either mapped uniquely or had exactly two alignments to B6 and PWD. For regions not correctly mapped in both B6 and PWD, this strategy automatically falls back to the represented reference. A correspondence map of chr5 of PWD scaffolds to mm10 (31) was used to derive exact corresponding positions,

Published OnlineFirst November 5, 2020; DOI: 10.1158/0008-5472.CAN-20-1480

including gaps and insertions, between PWD and B6 (Supplementary Fig. S1B and S1C).

RNA-seq analysis

Bam files were generated after aligning RNA-seq reads to the mixed reference using bwa (32) and mapping the PWD reads to their corresponding position in the mm10 (Supplementary Fig. S2). htseq-count (33) was used to count reads and DESeq2 (34) was used to call differential expression. To identify genes expressed differentially between the two alleles in heterozygous animals, we filtered for genes with ≥10 allele-specific reads and ≥90% assigned allele-specific reads. Next, allelic ratios were computed as the fraction of allele-specific reads originating from PWD. For single-sample gene set enrichment analyses (GSEA), we employed the R/Bioconductor package, GSVA, using gene sets in Supplementary Table S1. We extracted counts per each gene with at least 0.5 counts per million reads for each sample, and applied gsva with parameters min.sz = 5, max.sz = 500, mx.diff = TRUE, and kcdf = "Poisson."

MeDIP seq analysis

Immunoprecipitated methyl-DNA sequencing (MeDIP-seq) reads where aligned to the mixed reference using bwa, and PWD reads were transferred to the corresponding position in mm10. Differentially methylated regions (DMR) were called using QSEA (35). For allele-specific methylation analysis in C5F1 mice, we filtered for genomic regions with ≥10 allele-specific reads in the MeDIP data, and removed windows with <90% correctly assigned reads in parental strains. We calculated allelic ratios as the fraction of the allele-specific reads originating from PWD. Allelic methylation in C5F1 mice was computed as the log ratio of allele-specific reads to the mean of corresponding allelic reads in the parental strains (see Supplementary Fig. S3A for alignment statistics and Supplementary Fig. S3B for reference bias).

Comparison of human SNPs and PWD variants

To screen genetic variants in B6 versus PWD for human polymorphisms potentially affecting colon cancer susceptibility, we assembled human homologs of the chromosome 5 genes affected by PWD/B6 polymorphisms. Next, genes were screened for germline variants enriched in The Cancer Genome Atlas (TCGA) colon adenocarcinoma (COAD) cohort compared with general populations represented by the five 1000 Genomes superpopulations (EAS, East Asian; EUR, European; AFR, African,; AMR, Ad Mixed American; and SAS, South Asian; ref. 36). We applied a beta-binomial test on allele counts at all polymorphic sites passing the 1000 genome filter criteria. After adjustment for multiple testing, we selected genes with polymorphisms over- or underrepresented in TCGA COAD cohort compared with all superpopulations ($P_{adj} < 0.01$).

Data availability

The datasets supporting the conclusions of this article are available in Gene Expression Omnibus under GSE148368, GSE148369, and GSE148370. All further data and materials are available from the authors upon reasonable request.

Results

The PWD genome suppresses APC^{Min}-induced tumorigenesis

To test whether the PWD genetic background contains gene variants modifying intestinal tumor formation, we crossed B6-*Apc*$^{Min/+}$ mice with PWD mice and quantified the extent of intestinal tumor formation in F1 offspring animals at 15–19 weeks of age (**Fig. 1**; Supplementary Fig. S4A). B6-*Apc*$^{Min/+}$ animals developed on average 135.5 ± 44.3 (SD, $n = 43$ mice) macroscopically visible intestinal adenomas. In striking contrast, (B6xPWD)F1-*Apc*$^{Min/+}$ offspring developed only 6.4 ± 4.2 adenomas ($n = 13$), indicating that the PWD genome strongly suppresses intestinal tumor formation. Next, to test the effects of individual PWD chromosomes, we employed chromosome substitution strains (CSS) that are homozygous for single PWD chromosomes carried on the B6 genetic background (18). We crossed 10 CSSs with B6-*Apc*$^{Min/+}$ mice and scored offspring for intestinal adenoma. We found that the presence of a single copy of most PWD chromosomes tested resulted in significantly reduced tumor multiplicity compared with B6-*Apc*$^{Min/+}$. The effects of individual PWD chromosomes were generally weaker than those of the

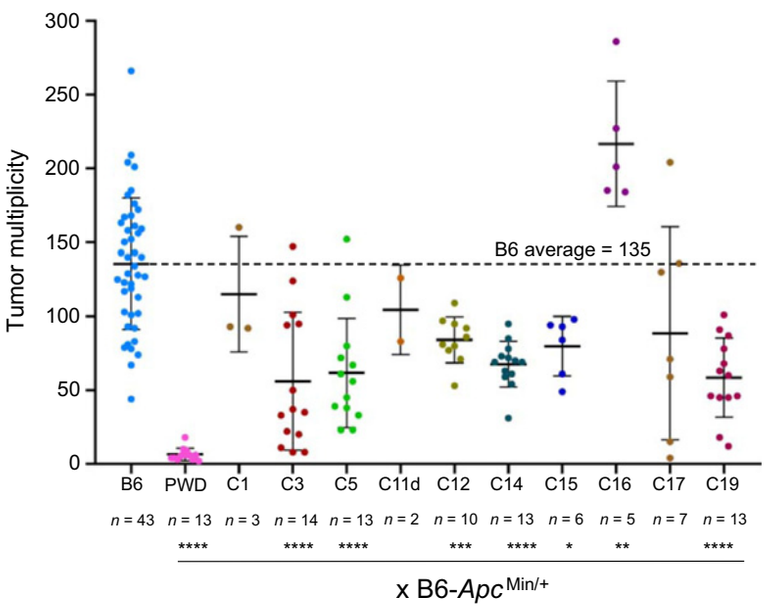

Figure 1.
The PWD genome contains multiple modifiers of *Apc*^{Min}. Tumor multiplicity in the intestines of B6-*Apc*$^{Min/+}$ mice or F1 *Apc*$^{Min/+}$ offspring of B6-*Apc*$^{Min/+}$ crossed with PWD or B6/PWD consomic strains (C1–C19) is given, as indicated. Graph indicates mean and SD of tumor multiplicity in the intestinal tract of mice of 15–19 weeks of age. Microscopically visible adenomas were counted. *, $P \leq 0.05$; **, $P \leq 0.01$; ***, $P \leq 0.001$; ****, $P \leq 0.0001$, respectively, using Mann–Whitney two-tailed significance tests.

Published OnlineFirst November 5, 2020; DOI: 10.1158/0008-5472.CAN-20-1480

complete PWD genome (**Fig. 1**). In a single case, a higher rate of tumor formation was observed.

For further analyses, we focused on chromosome 5 that reduced adenoma incidence to 64.1 ± 30.5 (n = 13 mice) in (B6xCSS5)F1-*Apc*$^{Min/+}$ mice (abbreviated as C5F1-*Apc*$^{Min/+}$). To distinguish between the activities of dominant tumor suppressor genes present on PWD chromosome 5 and dosage-dependent modifiers, we intercrossed C5F1-*Apc*$^{Min/+}$ and C5F1 mice and derived animals homozygous for PWD chromosome 5 on the B6 background carrying *Apc*$^{Min/+}$ (termed C5-*Apc*$^{Min/+}$). These mice displayed a further significant reduction of tumor load to 18.5 ± 9.3 adenomas (n = 8 mice; **Fig. 2A** and **B**; Supplementary Fig. S4B and S4C for tumor incidence in relation to sex or intestinal segment). Thus, PWD chromosome 5 can attenuate *Apc*^{Min}-dependent tumor formation in a dosage-dependent manner.

PWD chromosome 5 contains multiple tumor-suppressive loci

We crossed C5F1-*Apc*$^{Min/+}$ mice with parental B6 or the homozygous C5 consomic mice to generate *Apc*$^{Min/+}$ mice carrying parts of PWD chromosome 5. We assessed tumor multiplicity (phenotype) and chromosomal status using a panel of 35 SNP markers along chromosome 5 (genotype) to distinguish between B6 and PWD chromosomal contribution (18).

We used genotype and phenotype data of 105 *Apc*$^{Min/+}$ recombinant mice with single or multiple cross-overs on chromosome 5 for mapping of QTLs (29) and found that the logarithmic odds ratio (LOD) of marker linkage with tumor multiplicity was constantly high along the entire chromosome, with very high confidence (P < 0.0001; **Fig. 3A**). These data suggest that tumor multiplicity is controlled by multiple QTLs on chromosome 5, rather than by a single gene locus.

Next, we clustered genotype data of 184 mice with either complete B6 or PWD chromosomes 5 or various proportions of both and assigned the mice to 18 clusters representing similar allelic composition (**Fig. 3B**). We found significant differences in tumor multiplicity in mice assigned to different clusters (**Fig. 3C** and **D**), as assessed by two-tailed Mann–Whitney tests in pair-wise comparisons. The tumor-suppressive effect conferred by each subchromosomal region was smaller than the contribution of the complete PWD chromosome 5. Thus, we conclude that chromosome 5 contains a minimum of two, but likely many more genomic loci that additively affect intestinal tumor multiplicity in the mouse.

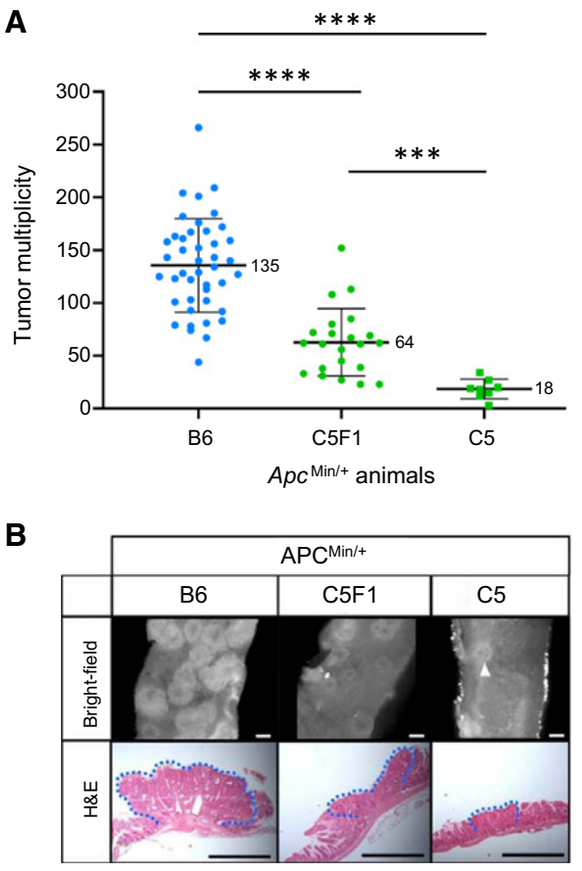

Figure 2.

PWD chromosome 5 suppresses tumor formation in *Apc*^{Min} mice in a dosage-dependent manner. **A,** Tumor multiplicity in intestines of B6-, C5-, and (B6 x C5) F1-*Apc*$^{Min/+}$ mice. Graph indicates mean and SD. ***, $P \leq$ 0.001; ****, $P \leq$ 0.0001, respectively, using Mann–Whitney two-tailed significance tests. **B,** Bright-field images of intestinal segments (ileum) and hematoxylin and eosin (H&E)-stained adenoma sections from B6-, C5-, and C5F1- APC$^{Min/+}$ mice as indicated. Scale bars, 1 mm.

Many candidate tumor suppressors on chromosome 5 are controlled in *cis*

Differences in gene expression levels can have a strong impact on phenotypic outcome. Therefore, we decided to investigate transcriptomic differences between tumor-prone and tumor-suppressive states. We generated triplicate transcriptomes from wild-type (*Apc*$^{+/+}$) and normal (*Apc*$^{Min/+}$) intestinal tissue, and from adenoma (usually containing *Apc*$^{Min/-}$ alleles due to loss of APC heterozygosity), derived from B6 and C5 mice, as well as from heterozygous C5F1 offspring. We mapped RNA sequence reads to a mixed reference consisting of the B6 mm10 mouse genome and a PWD genome assembly generated by us for this project (see Material and Methods; Supplementary Fig. S1). Principal component analysis revealed a separation between the nontumor intestine and adenoma transcriptomes along component 1, with B6 adenoma showing the greatest distance to wild-type tissue (**Fig. 4A**). Transcriptome differences corresponding to genetic background were less prominent and best reflected in component 4.

Transcriptome analysis revealed 174 genes showing significant expression differences in normal intestines between the groups. Of those, 58 genes were located on chromosome 5, representing putative modifier loci (**Fig. 4B**; Supplementary Table S2). The remaining 116 genes were encoded by other chromosomes (Supplementary Fig. S5; Supplementary Table S3).

The *cis*-control of modifier genes might be a mechanism to resist tumor initiation by the *Apc*^{Min} mutation. To determine the extent of *cis*- versus *trans*-regulation on chromosome 5, we assessed gene expression differences between C5 and PWD intestines, as well as between B6 and C5 intestines (**Fig. 4C**; refs. 37, 38). Similar numbers of genes were found to be regulated either in *cis* or in *trans*, and only a few genes were regulated by both *cis*- and *trans*-acting factors in PWD (Supplementary Table S4). Strikingly, among the 58 genes, which were differentially expressed between the normal intestine of mice carrying B6 or PWD chromosome 5 (**Fig. 4B**), 49 genes were *cis*-controlled. Moreover, for 47 of these, the PWD-encoded genes did not significantly change their expression level between wild-type *Apc*$^{+/+}$ or normal *Apc*$^{Min/+}$ intestine, nor in *Apc*$^{Min/-}$ adenoma, and may, therefore, counteract tumor-driving mechanisms triggered by *Apc*^{Min} or loss of *Apc*. These *cis*-controlled genes represent the prime candidates for suppressors of *Apc*^{Min}-induced tumor formation located on PWD chromosome 5 (Supplementary Table S5).

Published OnlineFirst November 5, 2020; DOI: 10.1158/0008-5472.CAN-20-1480

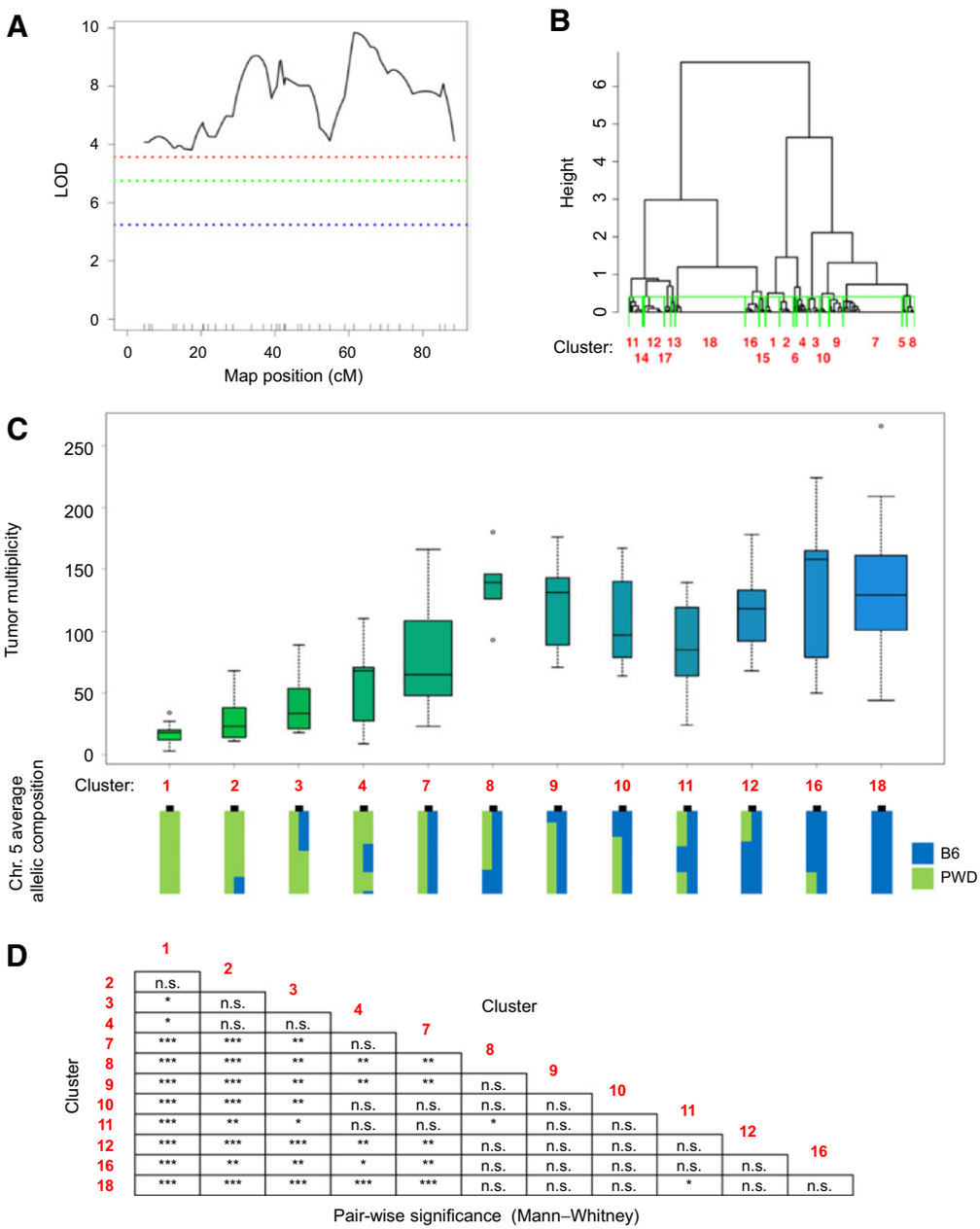

Figure 3.

PWD chromosome 5 contains multiple tumor-suppressive loci. **A,** Mapping of QTLs on chromosome (Chr.) 5, using genotypes and phenotypes (tumor multiplicity) of 105 *Apc*$^{Min/+}$ recombinant mice containing at least one crossing over between B6 and PWD chromosome 5. Figure shows LOD along chromosome 5, according to a panel of 35 polymorphic markers (positions indicated by vertical lines). Blue, green, and red dotted lines indicate confidence levels of $P = 0.01$, $P = 0.001$, and $P = 0.0001$, respectively. The confidence interval extends over the entire chromosome. **B,** Genotype-based hierarchical clustering of 184 *Apc*$^{Min/+}$ mice recombinant or nonrecombinant on chromosome 5 according to the panel of 35 polymorphic SNP markers as in **A**. Clustering resulted in 18 different clusters. Green marks and red numbers indicate 12 clusters with $\geq$ 5 mice that were used for further analyses. **C,** Correlation of phenotype (tumor multiplicity) and genotype across 12 clusters with $\geq$ 5 mice. Plot elements are defined as follows: lines in the boxes mark the median value. Boxes extend from the 25% to the 75% quantiles of the sample. Whiskers denote an additional 150% of the interquartile ranges. Width of boxes are proportional to the number of mice per cluster. Color gradient reflects the fraction of PWD (green) and B6 (blue) genotype across chromosome 5. Schematic representation of polymorphic SNP marker status along both chromosomes 5 in the different clusters (bottom). Centromere, indicated by black mark, located on top of the chromosome. **D,** Significances of differences in intestinal tumor load between the 12 genotype-based clusters of mice, using pair-wise Mann–Whitney significance tests. Red numbers on both axes indicate cluster numbers as defined in **B**. *, $P < 0.05$; **, $P < 0.01$; ***, $P < 0.001$; n.s., not significant ($P > 0.05$).

Published OnlineFirst November 5, 2020; DOI: 10.1158/0008-5472.CAN-20-1480

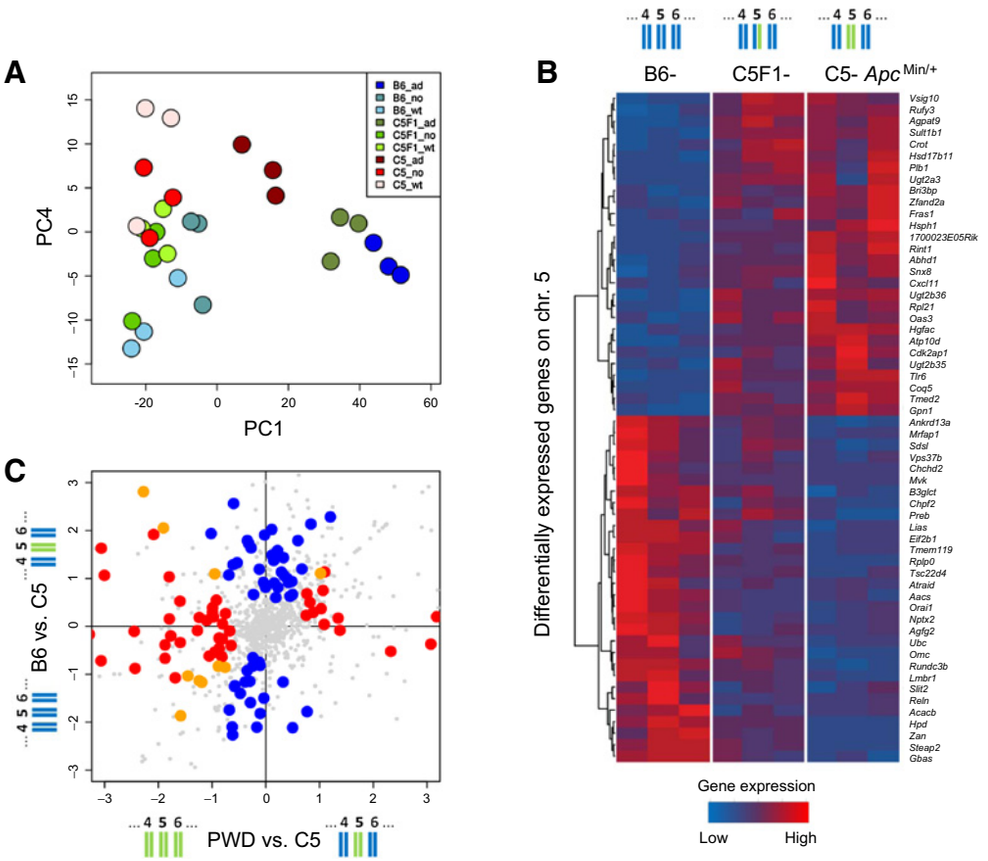

Figure 4.

Transcriptome analyses identified multiple *cis*-controlled modifier candidate genes. **A,** Principal component analysis of triplicate transcriptomes of wild-type, normal, and adenoma intestinal tissues derived from B6-, C5F1-, and C5- *Apc*$^{Min/+}$ mice. Shown are principal components 1 and 4. **B,** Gene expression heatmap of modifier candidate genes differentially expressed in the normal intestine of B6-, C5F1-, and C5-A*pc*$^{Min/+}$ mice and located on chromosome 5 (1.5-fold change, $P_{adj} < 0.01$ using DESeq2 with the nbinomWald test). **C,** Average $\log_2$ expression fold changes of chromosome 5 genes differentially expressed between B6 and C5 or PWD and C5 wild-type mice, respectively. Blue and red dots indicate genes showing significant *cis* or *trans* regulation, respectively (1.5-fold change, $P_{adj} < 0.01$ using DESeq2 with the nbinomWald test). Orange dots indicate genes with *cis* and *trans* regulation. **B** and **C,** Blue and green symbols represent B6 and PWD chromosomes, respectively.

Gene expression and DNA methylation in C5F1 animals are predominantly controlled in a parental allele-specific manner

We asked whether the gene expression levels and epigenetic modification patterns were inherited or adapted between B6 and PWD alleles, and investigated allele-specific gene transcription and epigenetic modification in the normal intestine of C5F1 *Apc*$^{Min/+}$ mice. We aligned transcriptome reads with strain-specific polymorphic sites to the mixed reference consisting of the B6 and PWD chromosomes 5 (Supplementary Fig. S2). We found a high correlation between parental gene expression and the expression of the corresponding alleles in offspring C5F1 mice (**Fig. 5A**), indicating that allelic expression in normal tissue mostly follows parental patterns. However, in consomic C5F1 adenoma, allele-specific expression was overall diminished, suggesting that the deregulation of cancer-associated gene expression networks partly obscures the expression of *cis*-controlled genes (**Fig. 5B**).

Because DNA methylation is a relatively stable epigenetic mark that has a strong impact on gene control, we tested whether the DNA methylation patterns of chromosome 5 in the C5F1 intestinal tissue resemble the patterns observed in the parental strains. We first identified 2,840 DMRs between B6 and PWD chromosome 5, by MeDIP-seq, and then determined allele-specific reads derived from each DMR (Supplementary Fig. S3A). We found that PWD-derived MeDIP-seq reads in C5F1 tissue were frequently enriched for hypermethylated DMRs and low among hypomethylated DMRs identified in PWD as compared with B6 tissue (**Fig. 5C**), and this pattern was unchanged in adenoma (**Fig. 5D**). Indeed, DMRs between B6 and C5 chromosome 5 remained strikingly stable in C5F1, by and large reflecting the parental (B6 and PWD) methylation patterns (**Fig. 5E**). The differential methylation between B6 and PWD may, in part, be explained by local differences in CpG density, as regions with methylation gains or losses between B6 and PWD were enriched in genomic windows with higher or lower numbers of CpGs, respectively (Supplementary Fig. S6A–S6C). We conclude that DNA methylation patterns remain quite stable between parents and offspring and are most frequently controlled in *cis*.

PWD chromosome 5 alters β-catenin and stemness expression signatures in the intestine

PWD-encoded modifiers might control *APC*^{Min} penetrance and tumor multiplicity via regulating stem cell numbers and Wnt/β-catenin signaling. We surveyed cell types of the intestinal crypt

Published OnlineFirst November 5, 2020; DOI: 10.1158/0008-5472.CAN-20-1480

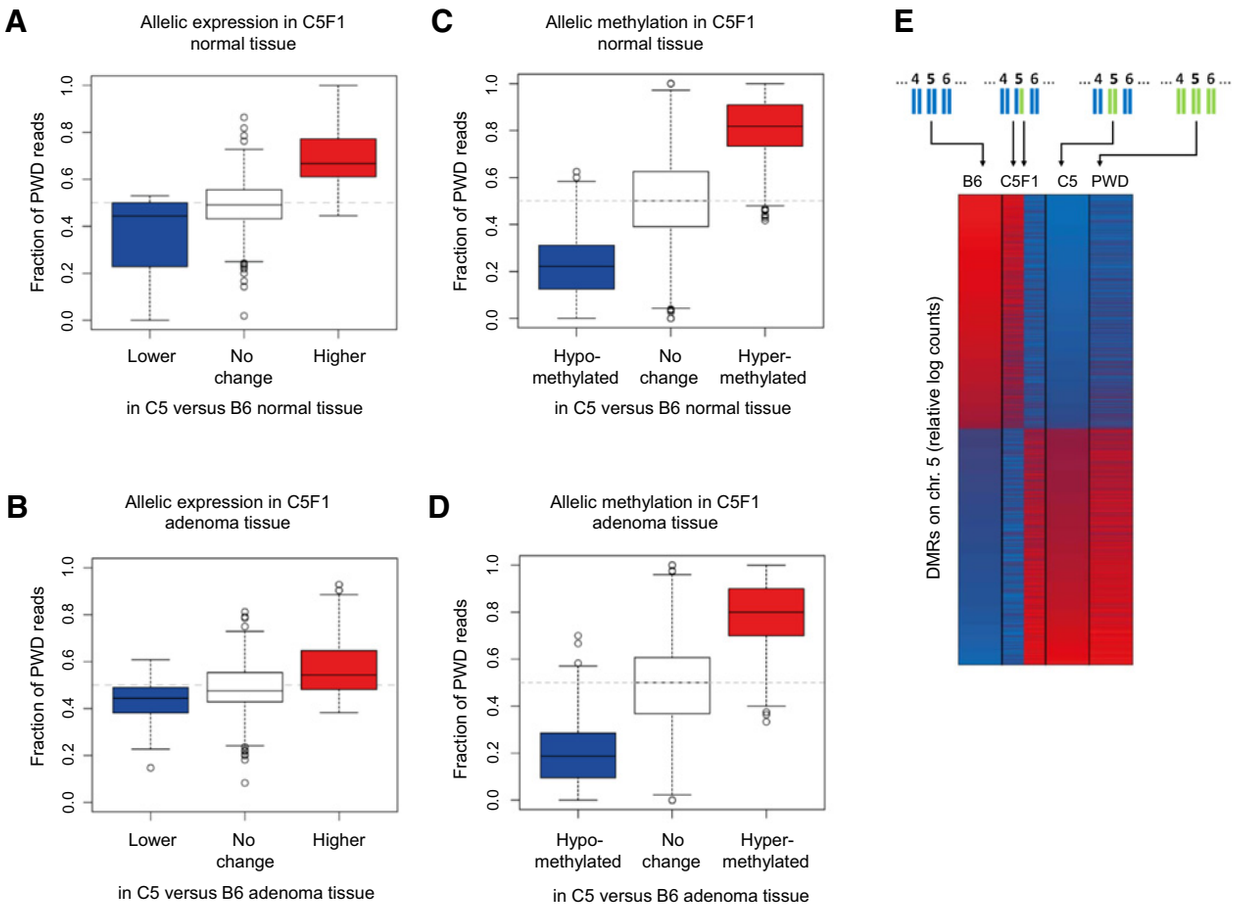

Figure 5.

Allelic gene expression and DNA methylation patterns in F1 mice are by and large inherited. **A–D,** Box plots showing allele-specific mapping of sequence reads with strain-specific polymorphisms. **A** and **B,** Fractions of PWD-specific RNA-seq reads in C5F1 intestines. Genes were grouped according to higher or lower expression in normal intestines (**A**) or adenoma (**B**) of parental C5 mice compared with B6, as indicated. **C** and **D,** Fractions of PWD-specific MeDIP-seq reads in C5F1 mice. Genomic regions were assigned to DMRs in C5 versus B6 mice, as indicated. **E,** Heatmap of MeDIP-seq read density in DMRs on chromosome 5 in normal intestines of mice, as indicated. Red and blue indicate high and low methylation, respectively. Blue and green symbols above diagram represent B6 and PWD chromosomes, respectively.

by ISH for the intestinal stem cell marker, *Olfm4*, and by IHC for the Paneth cell marker, Lyz (Supplementary Fig. S7), but observed no obvious differences between intestines of B6, C5F1, and C5 mice. For a quantitative assessment, we next analyzed functional gene expression modules comprising target genes of the Wnt/β-catenin and ERK pathways relevant for intestinal tumor formation (39, 40) and intestinal cell differentiation programs (41–43), using GSEA (for signatures, see Supplementary Table S1; ref. 44). We found that the expression of β-catenin (WNT) target genes was increased in adenoma, compared with wild-type or normal intestine (**Fig. 6A**). However, this increase was much weaker in C5 adenoma when compared with adenoma derived from the tumor-prone B6 mice. In contrast, ERK target genes were upregulated in adenoma across all genetic backgrounds. The expression of stem cell and transiently amplifying cell markers was increased in adenoma compared with normal intestines, as expected, but again the increase was much stronger in B6 than in C5 mice. These data suggest that C5 adenoma maintains a more balanced ratio of stem cell- to differentiation-related gene expression programs, compared with B6 adenoma.

To extend these observations to nonmalignant wild-type $Apc^{+/+}$ versus normal $Apc^{Min/+}$ intestinal tissues, we performed pair-wise comparisons across the genotypes. In tumor-prone B6-$Apc^{Min/+}$ mice, we observed increased expression of β-catenin targets and stem cell signature genes already in the normal intestines when compared with wild-type $Apc^{+/+}$ intestines (**Fig. 6B**). This likely results from the fact that the Apc^{Min} allele encodes a truncated protein, which can compete with wild-type APC for binding to the β-catenin degradation complex (45). In contrast, such differences were not found in $Apc^{+/+}$ versus $Apc^{Min/+}$ mice containing one (C5F1) or two (C5) PWD copies of chromosome 5. These data indicate that PWD gene variants on chromosome 5 specifically maintain moderate β-catenin activity despite the Wnt-promoting action of the Apc^{Min} allele and can, therefore, counteract the tumor-promoting effects of the Apc^{Min} driver mutation on the β-catenin–driven expansion of the stem cell pool.

Organotypic cultures identify cell intrinsic differences between B6 and C5F1 adenomatous spheroids

To test whether the transcriptional differences observed between B6 and C5 intestines were tissue intrinsic, we established organoid

Published OnlineFirst November 5, 2020; DOI: 10.1158/0008-5472.CAN-20-1480

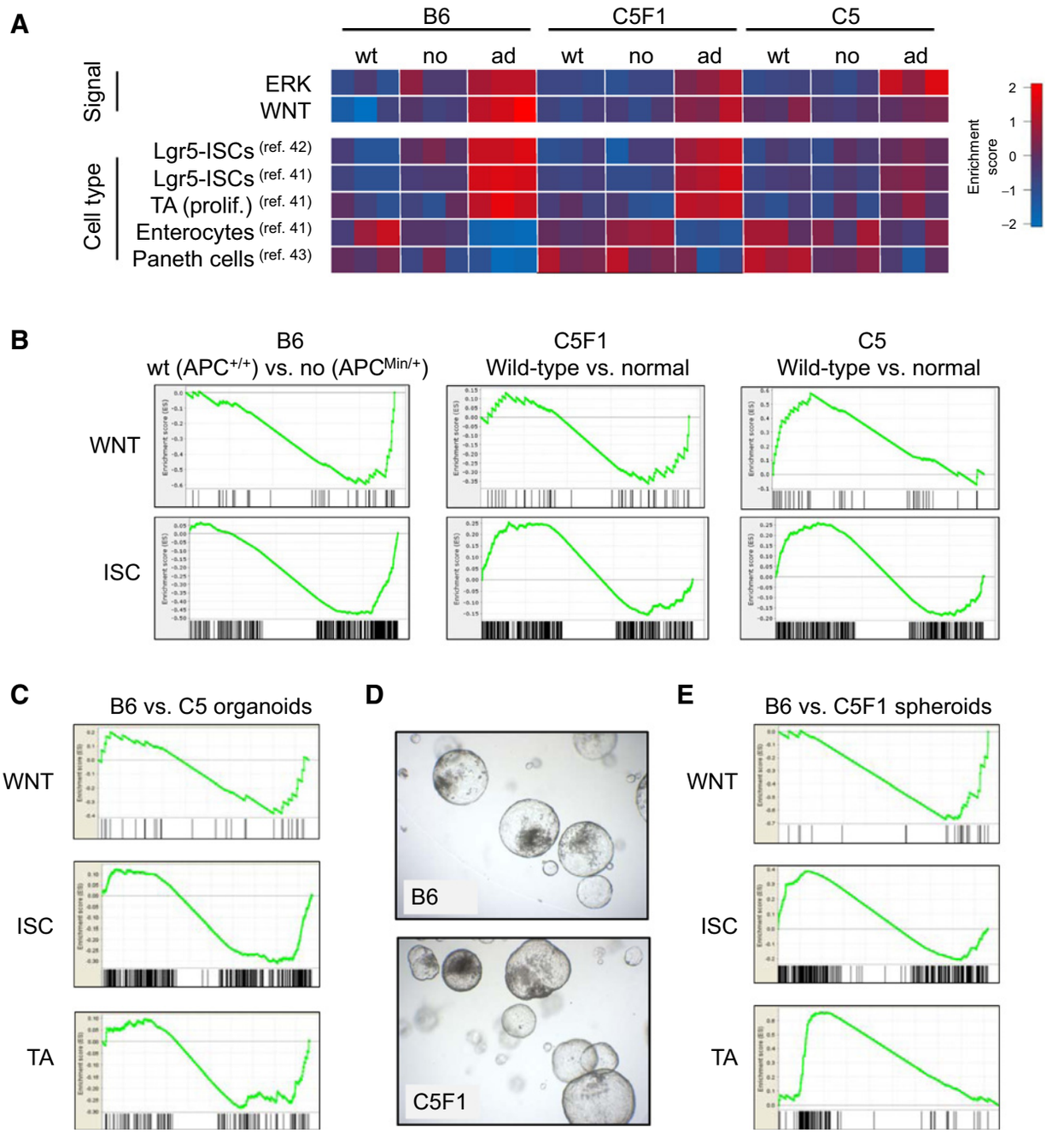

Figure 6.

PWD chromosome 5 alters gene expression signatures related to intestinal adenoma (ad) initiation. **A,** Heatmap of enrichment scores for signaling and cell type gene expression signatures in intestinal tissues, as indicated. ERK and WNT signatures comprise target genes of the signaling pathways. Lgr5-ISC indicates genes predominantly expressed in Lgr5-driven intestinal stem cells (ISC), whereas transiently amplifying (TA), enterocyte, and Paneth cell signatures comprise genes predominantly expressed in transiently amplifying proliferative cells, differentiated absorptive enterocytes, or secretory-lineage Paneth cells, respectively. References for the cell type signatures are given in the figure. Red and blue indicate high and low relative signature activity, respectively, as determined by single sample GSEA. **B**, **C**, and **E,** Comparative GSEA of tissues and signatures as indicated. **D,** Bright-field images of spheroids derived from B6 or C5F1 adenoma tissue, as indicated. no, normal; wt, wild-type.

cultures from wild-type B6 and C5 intestine (19). We found that organoids were phenotypically indistinguishable. Analysis of duplicate transcriptomes from B6 versus C5 organoids by GSEA yielded no significant differences in the expression of β-catenin targets, nor in the expression of marker genes for stem, proliferative, or differentiated cell types (**Fig. 6C**), in-line with transcriptome comparisons of B6 versus C5 wild-type intestines, which were also very similar (see above; **Fig. 4A**).

Published OnlineFirst November 5, 2020; DOI: 10.1158/0008-5472.CAN-20-1480

We next derived organoid cultures from adenoma cells, using exclusively the growth factors EGF and noggin, thus selecting specifically for adenomatous cells. Adenoma cultures established from B6 grew as perfect spherical structures, as reported previously (**Fig. 6D**; refs. 19, 46). In contrast, adenoma cells derived from C5F1 mice formed more irregular structures. RNA-seq followed by GSEA revealed a somewhat stronger expression of Wnt/β-catenin targets in C5F1 as compared with B6 spheroids, unlike the analysis of *in vivo* adenoma (**Fig. 6E**). However, stem cell signatures were not significantly different. In contrast, the B6 spheroids displayed a stronger transiently amplifying cell proliferative signature compared with C5F1. The data confirm that part of the differences between adenoma tissue derived from B6 as compared with C5F1 or C5 mice are cell intrinsic, but also suggest the existence of additional levels of adenoma growth regulation *in vivo*, for instance by the stromal microenvironment.

Particular variants of eight human genes are depleted in colorectal cancer

We extended our analysis to human orthologs of the murine chromosome 5 candidate genes, located mainly in syntenic regions on human chromosomes 4, 7, and 12 (see Supplementary Table S6 for information on syntenic regions). We first mapped polymorphisms between B6 and PWD in coding regions and identified 2,103 amino acid differences in 678 genes (of a total of 1,370 located on chromosome 5) encoding protein variants with nonsynonymous amino acid changes, frameshifts, or nonconserved stop codons. Of those, 431 genes were expressed either in the mouse normal intestine or adenoma (**Fig. 7A**; Supplementary Table S7)

Next, we analyzed whether variant alleles of these genes were over- or underrepresented in patients with colorectal cancer. For this, we identified the human orthologs of the 431 variant chromosome 5 genes identified in mice and compared SNP frequencies of these orthologs in the germline of more than 300 patients with colorectal cancer with SNP frequencies in the general population, using data available in TCGA (47) and dbSNP (48). We excluded SNPs with an excessive heterozygous allele frequency, which might be due to sequencing or mapping artifacts (49), and gave priority to SNPs that showed consistent allele frequency differences between genomes of patients with colorectal cancer and the five human superpopulations in dbSNP, representing genomes of African, American, East Asian, European, and South Asian origin (**Fig. 7B**). Among those, we identified moderate effect SNPs (i.e., causing missense mutations; see Supplementary Table S6), which were strongly underrepresented in patients with colorectal cancer as compared with the general population ($P_{adj} < 0.01$). These SNPs defined allelic variants of eight genes: *ATXN2, EMILIN1, USP42, AKAP9, KIAA1211, TNRC18, NOM1*, and *SOWAHB*. Our data reveal a depletion of particular gene variants among patients with colorectal cancer, suggesting that these variants might counteract colorectal cancer development.

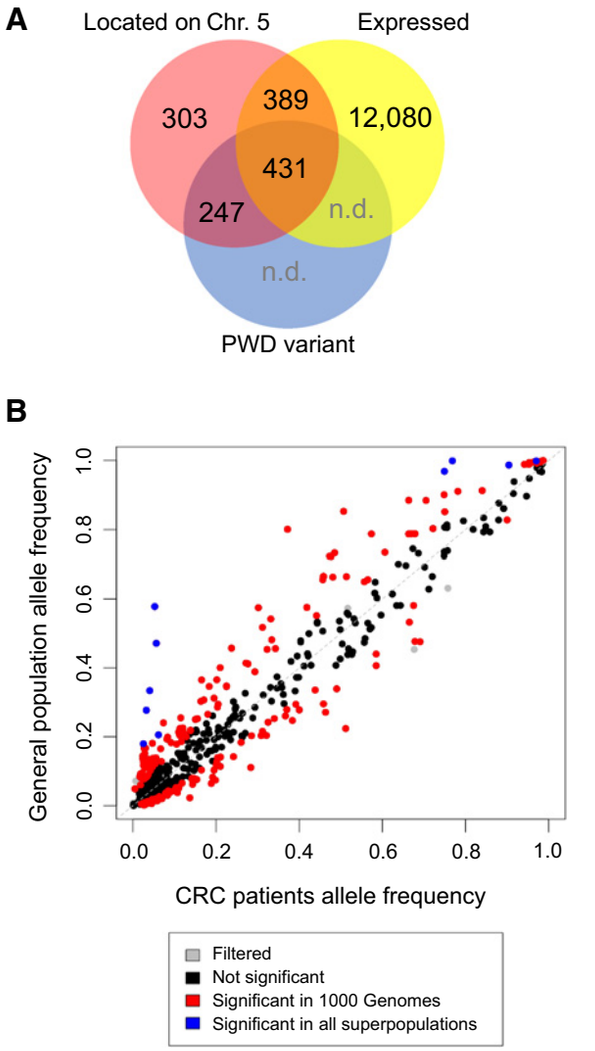

Figure 7.
Identification of orthologue human protein variants depleted in human patients with colorectal cancer. **A,** Venn diagram showing overlap between genes located on mouse chromosome (Chr.) 5 (red), expressed in the mouse intestine (yellow), or encoding protein variants between B6 and PWD (blue). **B,** Differential allele frequencies of 582 SNPs occurring in human orthologues of 431 murine candidate genes detected in patients with colorectal cancer (CRC; TCGA database) as compared with the general population (1000 Genomes database). Data points marked in red represent SNPs significantly different in a comparison between patients with colorectal cancer and the general population, as judged by a beta-binomial test, while SNPs marked in blue are, in addition, significant across comparisons between genomes of patients with colorectal cancer and all five human superpopulations, as defined by the 1000 Genomes Project (36). For gene names and allele details, see Supplementary Table S6. n.d., not determined.

Discussion

We have analyzed intestinal tumor multiplicity, gene expression, and DNA methylation in CSSs of B6 and PWD mice. We found that B6 mice are permissive, while PWD mice are largely suppressive toward tumor formation triggered by Apc^{Min}. Tumor-suppressive factors are distributed over many PWD chromosomes. On PWD chromosome 5 alone we identified at least two tumor-suppressive loci acting in a dosage-dependent manner and multiple *cis*-regulated PWD gene variants most likely contributing to tumor suppression. We showed that PWD chromosome 5 alters signaling networks responsible for colorectal cancer formation, in particular by maintaining moderate Wnt/β-catenin activity.

Multiple mechanisms affecting β-catenin activity, which may contribute to the differential response to *Apc* loss in B6, C5F1, or C5 mice, have been described previously (50, 51). On the B6 genetic background, upregulation of Wnt/β-catenin activity following *Apc* loss may result in higher rates of fixation and clonal expansion of $Apc^{Min/-}$

cells (52, 53). Fixation, that is, spreading of mutant stem cell progeny throughout a crypt, appears to be a rate-limiting step in the formation of colorectal cancer in humans (54).

We suggest that differential modifier effects, as seen in C5 versus B6 mice in this study, may also impact on individual tumor risk in humans. Support for this notion comes from the finding that the same *APC* mutation can result in highly variable numbers of adenoma in humans (55).

Our study suggests that modifiers of Min primarily interact with the Wnt/β-catenin signaling network controlling the intestinal crypt. This is in agreement with recent data identifying *Pla2g2a* (also known as *Modifier of APC^{Min} 1, Mom1*) as an intestinal stem cell niche factor regulating intestinal tumor multiplicity via Wnt/β-Catenin activity (56). Moreover, several modifier candidate genes located on chromosome 5 that we found to be expressed at lower level in C5 mice compared with B6 have previously been linked to the control of Wnt signaling (see also **Fig. 4B**): *Reln* (encoding Reelin), is a signal transducer interacting with Wnt/β-catenin (57). *Slit2* promotes intestinal tumorigenesis through Src-mediated activation of β-catenin (58). *Rundc3b* encodes a protein binding the β-catenin stability-regulating casein kinase 1 gamma 1/2 (59). *Mvk*, encoding a kinase of the mevalonate pathway, interacts with oncogenic signaling networks controlling cell differentiation programs (60). However, the actual roles in tumor suppression of all modifier candidates identified in this work remain to be established, and multiple mechanisms may be involved.

Our data reveal a class of putative modifier genes, which are *cis*-controlled and do not significantly change their expression level between wild-type and *Apc*^{Min}-affected tissue, nor in adenoma. Moreover, they do not significantly change their expression levels from parents to offspring, and thus, represent heritable invariable components of gene networks, which may play a pivotal role in creating phenotypic differences between individuals. Strikingly, on PWD chromosome 5 alone we have identified 47 such genes, which are differentially expressed between B6 and PWD in the intestine. Genes of that kind, that is, genes unaffected by distortion of regulatory networks, might act on multiple levels, as indicated by the variety of candidate modifier genes shown in **Fig. 4**B. Extrapolating from the number of modifier candidates detected on chromosome 5, we estimate that across the genome at least several 100 gene variants may contribute to the tumor-suppressive effect observed in (B6xPWD)F1-*Apc*$^{Min/+}$ mice, protein variants not even considered. This estimate demonstrates the dimension of gene loci and variants involved in tumor formation or suppression. In addition, we observed high conservation in the DNA methylation patterns between parents and offspring, providing an epigenetic basis for the inheritance of invariant gene expression of at least a subset of gene variants, which may act as modifiers.

It has been suggested that a major risk factor for cancer is the occurrence of random mutations arising during DNA replication in adult stem cells (3). Human colon cancer is known to be strongly affected by hereditary components. However, despite many genome-wide association studies, few gene variants have been shown to influence the risk of sporadic colorectal cancer (61). The reason for this may be that sporadic colorectal cancer incidence might be controlled by many loci with small effects. Further studies combining candidate gene approaches in mice and assessment of allele frequencies in human populations might be applicable for pinpointing tumor-protective genetic variants in humans, although this approach might be hampered by physiologic differences between the mouse small intestine and the human colon.

Here, we highlight an important factor affecting the individual risk for developing cancer: the genetic constitution of the individual. We show that the genetic predisposition can also mean that the genome provides a tumor-protective state by encoding particularly robust signaling networks comprising a multitude of genetic variants, which may synergize and withstand the effects of strong driver mutations. Future studies need to put particular emphasis on tumor-protective mechanisms encoded by the genome, which eventually might lead to individualized schemes for cancer screening or the development of new drugs enforcing signaling states protective against cancer.

Authors' Disclosures

C. Grimm reports grants from NGFN-Plus during the conduct of the study, as well as a patent for method for the diagnosis of colon cancer issued. R. Herwig reports grants from German Federal Ministry for Education and Research during the conduct of the study. B.G. Herrmann reports grants from German Ministry of Science and Education, grant no. PKT-01GS08111 during the conduct of the study. M. Morkel reports grants from German Ministry of Science and Education, grant no. PKT-01GS08111 during the conduct of the study. No disclosures were reported by the other authors.

Authors' Contributions

A.L. Farrall: Formal analysis, validation, investigation. **M. Lienhard:** Data curation, formal analysis, methodology. **C. Grimm:** Investigation. **H. Kuhl:** Data curation, methodology. **S.H.M. Sluka:** Investigation. **M. Caparros:** Investigation. **J. Forejt:** Resources. **B. Timmermann:** Resources. **R. Herwig:** Formal analysis, methodology. **B.G. Herrmann:** Conceptualization, formal analysis, supervision, funding acquisition, writing-original draft, writing-review and editing. **M. Morkel:** Conceptualization, formal analysis, supervision, funding acquisition, investigation, writing-original draft, writing-review and editing.

Acknowledgments

The authors wish to thank Sona Gregorova (Academy of Sciences of the Czech Republic) for help with import of mouse strains, Sonja Banko, Miriam Peetz, and many other mouse technicians at the MPIMG animal facility for mouse husbandry, Ursula Schulz (MPIMG) for help with dissections, Gaby Bläss (MPIMG) for RNA ISHs on tissue sections, and Yana Ruchiy and Philip Bischoff (Charité – Universitätsmedizin Berlin) for help with histology. The authors acknowledge funding for part of the study by German Ministry of Science and Education NGFNplus (PKT-01GS08111 to B.G. Herrmann and M. Morkel). A.L. Farrall was funded by a Max Planck Postdoctoral Research Fellowship.

The costs of publication of this article were defrayed in part by the payment of page charges. This article must therefore be hereby marked *advertisement* in accordance with 18 U.S.C. Section 1734 solely to indicate this fact.

Received May 5, 2020; revised August 26, 2020; accepted October 15, 2020; published first November 5, 2020.

References

1. Fearon ER. Molecular genetics of colorectal cancer. Annu Rev Pathol 2011;6:479–507.
2. van de Wetering M, Sancho E, Verweij C, de Lau W, Oving I, Hurlstone A, et al. The beta-catenin/TCF-4 complex imposes a crypt progenitor phenotype on colorectal cancer cells. Cell 2002;111:241–50.
3. Tomasetti C, Li L, Vogelstein B. Stem cell divisions, somatic mutations, cancer etiology, and cancer prevention. Science 2017;355:1330–4.
4. Groden J, Thliveris A, Samowitz W, Carlson M, Gelbert L, Albertsen H, et al. Identification and characterization of the familial adenomatous polyposis coli gene. Cell 1991;66:589–600.

5. Kinzler KW, Nilbert MC, Su LK, Vogelstein B, Bryan TM, Levy DB, et al. Identification of FAP locus genes from chromosome 5q21. Science 1991;253:661–5.
6. Nishisho I, Nakamura Y, Miyoshi Y, Miki Y, Ando H, Horii A, et al. Mutations of chromosome 5q21 genes in FAP and colorectal cancer patients. Science 1991;253:665–9.
7. De Jong MM, Nolte IM, Te Meerman GJ, Van der Graaf WTA, De Vries EGE, Sijmons RH, et al. Low-penetrance genes and their involvement in colorectal cancer susceptibility. Cancer Epidemiol Biomarkers Prev 2002;11:1132–52.
8. Valle L. Genetic predisposition to colorectal cancer: where we stand and future perspectives. World J Gastroenterol 2014;20:9828–49.
9. Lichtenstein P, Holm NV, Verkasalo PK, Iliadou A, Kaprio J, Koskenvuo M, et al. Environmental & heritable factors in the causation of cancer. N Engl J Med 2000;343:78–85.
10. Dragani TA. 10 years of mouse cancer modifier loci: human relevance. Cancer Res 2003;63;3011–8.
11. Nadeau JH. Modifier genes and protective alleles in humans and mice. Curr Opin Genet Dev 2003;13:290–5.
12. Demant P. Cancer susceptibility in the mouse: genetics, biology and implications for human cancer. Nat Rev Genet 2003;4:721–34.
13. Hamilton BA, Yu BD. Modifier genes and the plasticity of genetic networks in mice. PLoS Genet 2012;8:e1002644.
14. Moser AR, Pitot HC, Dove WF. A dominant mutation that predisposes to multiple intestinal neoplasia in the mouse. Science 1990;247:322–4.
15. Su LK, Kinzler KW, Vogelstein B, Preisinger AC, Moser AR, Luongo C, et al. Multiple intestinal neoplasia caused by a mutation in the murine homolog of the APC gene. Science 1992;256:668–70.
16. Leystra AA, Clapper ML. Gut microbiota influences experimental outcomes in mouse models of colorectal cancer. Genes 2019;10:900.
17. Moser AR, Dove WF, Roth KA, Gordon JI. The Min (multiple intestinal neoplasia) mutation: its effect on gut epithelial cell differentiation and interaction with a modifier system. J Cell Biol 1992;116:1517–26.
18. Gregorová S, Divina P, Storchova R, Trachtulec Z, Fotopulosova V, Svenson KL, et al. Mouse consomic strains: exploiting genetic divergence between *Mus m. musculus* and *Mus m. domesticus* subspecies. Genome Res 2008;18:509–15.
19. Sato T, Stange DE, Ferrante M, Vries RGJ, van Es JH, van den Brink S, et al. Long-term expansion of epithelial organoids from human colon, adenoma, adenocarcinoma, and Barrett's epithelium. Gastroenterology 2011;141:1762–72.
20. Parkhomchuk D, Borodina T, Amstislavskiy V, Banaru M, Hallen L, Krobitsch S, et al. Transcriptome analysis by strand-specific sequencing of complementary DNA. Nucleic Acids Res 2009;37:e123.
21. Grimm C, Adjaye J. Analysis of the methylome of human embryonic stem cells employing methylated DNA immunoprecipitation coupled to next-generation sequencing. Methods Mol Biol 2012;873:281–95.
22. Peng Y, Leung HCM, Yiu SM, Chin FYL. IDBA-UD: a *de novo* assembler for single-cell and metagenomic sequencing data with highly uneven depth. Bioinformatics 2012;28:1420–8.
23. Reinhardt JA, Baltrus DA, Nishimura MT, Jeck WR, Jones CD, Dangl JL. *De novo* assembly using low-coverage short read sequence data from the rice pathogen *Pseudomonas syringa*e pv. oryzae. Genome Res 2009;19:294–305.
24. Boetzer M, Henkel CV, Jansen HJ, Butler D, Pirovano W. Scaffolding preassembled contigs using SSPACE. Bioinformatics 2011;27:578–9.
25. Kajitani R, Toshimoto K, Noguchi H, Toyoda A, Ogura Y, Okuno M, et al. Efficient *de novo* assembly of highly heterozygous genomes from whole-genome shotgun short reads. Genome Res 2014;24:1384–95.
26. Luo R, Liu B, Xie Y, Li Z, Huang W, Yuan J, et al. SOAPdenovo2: an empirically improved memory-efficient short-read de novo assembler. Gigascience 2012;1:18.
27. Frith MC, Kawaguchi R. Split-alignment of genomes finds orthologies more accurately. Genome Biol 2015;16:106.
28. Kolmogorov M, Raney B, Paten B, Pham S. Ragout - a reference-assisted assembly tool for bacterial genomes. Bioinformatics 2014;30::i302–9.
29. Broman KW, Wu H, Sen S´, Churchill GA. R/qtl: QTL mapping in experimental crosses. Bioinformatics 2003;19:889–90.
30. Cox A, Ackert-Bicknell CL, Dumont BL, Yueming D, Bell JT, Brockmann GA, et al. A new standard genetic map for the laboratory mouse. Genetics 2009;182;1335–44.
31. Kieøbasa SM, Wan R, Sato K, Horton P, Frith MC. Adaptive seeds tame genomic sequence comparison. Genome Res 2011;21:487–93.
32. Li H, Durbin R. Fast and accurate long-read alignment with Burrows-Wheeler transform. Bioinformatics 2010;26:589–95.
33. Anders S, Pyl PT, Huber W. HTSeq–a Python framework to work with high-throughput sequencing data. Bioinformatics 2015;31:166–9.
34. Love MI, Huber W, Anders S. Moderated estimation of fold change and dispersion for RNA-seq data with DESeq2. Genome Biol 2014;15:1–21.
35. Lienhard M, Grasse S, Rolff J, Frese S, Schirmer U, Becker M, et al. QSEA-modelling of genome-wide DNA methylation from sequencing enrichment experiments. Nucleic Acids Res 2017;45:e44.
36. 1000 Genomes Project Consortium, Auton A, Brooks LD, Durbin RM, Garrison EP, Kang HM, et al. A global reference for human genetic variation. Nature 2015;526:68–74.
37. Goncalves A, Leigh-Brown S, Thybert D, Stefflova K, Turro E, Flicek P, et al. Extensive compensatory cis-trans regulation in the evolution of mouse gene expression. Genome Res 2012;22:2376–84.
38. Wong ES, Schmitt BM, Kazachenka A, Thybert D, Redmond A, Connor F, et al. Interplay of cis and trans mechanisms driving transcription factor binding and gene expression evolution. Nat Commun 2017;8:1092.
39. Liberzon A, Birger C, Thorvaldsdóttir H, Ghandi M, Mesirov JP, Tamayo P. The molecular signatures database hallmark gene set collection. Cell Syst 2015;1:417–25.
40. Uhlitz F, Sieber A, Wyler E, Fritsche-Guenther R, Meisig J, Landthaler M, et al. An immediate–late gene expression module decodes ERK signal duration. Mol Syst Biol 2017;13:928.
41. Merlos-Suárez A, Barriga FM, Jung P, Iglesias M, Céspedes MV, Rossell D, et al. The intestinal stem cell signature identifies colorectal cancer stem cells and predicts disease relapse. Cell Stem Cell 2011;8:511–24.
42. Muñoz J, Stange DE, Schepers AG, van de Wetering M, Koo B-K, Itzkovitz S, et al. The Lgr5 intestinal stem cell signature: robust expression of proposed quiescent "+4" cell markers. EMBO J 2012;31:3079–91.
43. Sato T, van Es JH, Snippert HJ, Stange DE, Vries RG, van den Born M, et al. Paneth cells constitute the niche for Lgr5 stem cells in intestinal crypts. Nature. 2010;469:415–8.
44. Subramanian A, Tamayo P, Mootha VK, Mukherjee S, Ebert BL, Gillette MA, et al. Gene set enrichment analysis: a knowledge-based approach for interpreting genome-wide expression profiles. Proc Natl Acad Sci U S A 2005;102:15545–50.
45. Kielman MF, Rindapää M, Gaspar C, Van Poppel N, Breukell C, Van Leeuwen S, et al. Apc modulates embryonic stem-cell differentiation by controlling the dosage of β-catenin signaling. Nat Genet 2002;32:594–605.
46. Farrall AL, Riemer P, Leushacke M, Sreekumar A, Grimm C, Herrmann BG, et al. Wnt and BMP signals control intestinal adenoma cell fates. Int J cancer 2012;131:2242–52.
47. The Cancer Genome Atlas Network. Comprehensive molecular characterization of human colon and rectal cancer. Nature 2012;487:330–7.
48. Sherry ST. dbSNP: the NCBI database of genetic variation. Nucleic Acids Res 2001;29:308–11.
49. Maruki T, Lynch M. Genotype-frequency estimation from high-throughput sequencing data. Genetics 2015;201:473–86.
50. Phelps RA, Chidester S, Dehghanizadeh S, Phelps J, Sandoval IT, Rai K, et al. A two-step model for colon adenoma initiation and progression caused by APC loss. Cell 2009;137:623–34.
51. Mieszczanek J, van Tienen LM, Ibrahim AEK, Winton DJ, Bienz M. Bcl9 and Pygo synergise downstream of Apc to effect intestinal neoplasia in FAP mouse models. Nat Commun 2019;10:724.
52. Vermeulen L, Morrissey E, van der Heijden M, Nicholson AM, Sottoriva A, Buczacki S, et al. Defining stem cell dynamics in models of intestinal tumor initiation. Science 2013;342:995–8.
53. Snippert HJ, Schepers AG, Van Es JH, Simons BD, Clevers H. Biased competition between Lgr5 intestinal stem cells driven by oncogenic mutation induces clonal expansion. EMBO Rep 2014;15:62–9.
54. Nicholson AM, Olpe C, Hoyle A, Wilkinson M, Morrissey E, Winton DJ, et al. Fixation and spread of somatic mutations in adult human colonic epithelium. Cell Stem Cell 2018;22:909–18.
55. Burt RW, Leppert MF, Slattery ML, Samowitz WS, Spirio LN, Kerber RA, et al. Genetic testing and phenotype in a large kindred with attenuated familial adenomatous polyposis. Gastroenterology 2004;127:444–51.
56. Schewe M, Franken PF, Sacchetti A, Schmitt M, Joosten R, Böttcher R, et al. Secreted phospholipases A2 are intestinal stem cell niche factors with distinct

roles in homeostasis, inflammation, and cancer. Cell Stem Cell 2016;19: 38–51.
57. Reiner O, Sapir T. Similarities and differences between the Wnt and reelin pathways in the forming brain. Mol Neurobiol 2005;31:117–34.
58. Zhang Q-Q, Zhou D-L, Lei Y, Zheng L, Chen S-X, Gou H-J, et al. Slit2/Robo1 signaling promotes intestinal tumorigenesis through Src-mediated activation of the Wnt/β-catenin pathway. Oncotarget 2015;6:3123–35.
59. Vinayagam A, Stelzl U, Foulle R, Plassmann S, Zenkner M, Timm J, et al. A directed protein interaction network for investigating intracellular signal transduction. Sci Signal 2011;4:rs8.
60. Gruenbacher G, Thurnher M. Mevalonate metabolism in immuno-oncology. Front Immunol 2017;10:77–85.
61. Tenesa A, Dunlop MG. New insights into the aetiology of colorectal cancer from genome-wide association studies. Nat Rev Genet 2009;10:353–8.

Published OnlineFirst November 5, 2020; DOI: 10.1158/0008-5472.CAN-20-1480

Cancer Research
The Journal of Cancer Research (1916–1930) | The American Journal of Cancer (1931–1940)

AACR American Association for Cancer Research

PWD/Ph-Encoded Genetic Variants Modulate the Cellular Wnt/β-Catenin Response to Suppress *Apc*^{Min}-Triggered Intestinal Tumor Formation

Alexandra L. Farrall, Matthias Lienhard, Christina Grimm, et al.

Cancer Res 2021;81:38-49. Published OnlineFirst November 5, 2020.